Electronic Supplementary Material (ESI) for ChemComm.

Supplementary Data

Rational Design of Hybridization Chain Reaction Monomers for Robust Signal Amplification

Yan Shan Ang and Lin Yue Lanry Yung*

Department of Chemical and Biomolecular Engineering, National University of Singapore, 10 Kent Ridge Crescent, Singapore 119260

*Corresponding author (cheyly@nus.edu.sg)

Table of Content

S1. Detailed Materials and Methods

Materials. All DNA oligonucleotides used in this study were purchased from Integrated DNA Technologies (IDT), and HPLC purified by IDT. The actual sequences used are shown in Table S1. The lyophilized DNA was reconstituted in 1X Tris-EDTA buffer (1X TE, pH 8.0) to give 100 μM stock and stored at 4 °C, except for Cy3/Cy5-modified DNAs which were stored at – 20 °C and protected from light. The sequences are provided in Table S1.

The following chemicals were used as received:

1X TE (pH 8.0): 1st BASE, cat. # BUF-3020-1X1L

10X Tris-borate-EDTA (TBE, pH 8.3): Vivantis, cat. # PB1040-1L

Agarose (molecular biology grade): Vivantis, cat. # PC0701-500G

DNA gel loading dye (6X): Thermo Scientific, cat. # R0611

Fetal bovine serum (Hyclone): Thermo Scientific, cat. # SV30160.03

Gene ruler ultra low range DNA ladder: Thermo Scientific, cat. # SM1211

Hydrochloric acid (1.0 N): Sigma Aldrich, cat. # 38282-1EA

Magnesium chloride ($MgCl_2$, ≥ 98%): Sigma Aldrich, cat. # M8266-100G

Sodium citrate tribasic dehydrate ($HOC(COONa)(CH_2COONa)_2 \cdot 2H2O$, ≥ 99.0%): Sigma Aldrich, cat. # S4641-500G

Sodium chloride (NaCl, ≥ 99.5%): Sigma Aldrich, cat. # 746398

SYBR gold nucleic acid stain (10 000X in DMSO): Invitrogen, cat. # S-11494

Tween-20: Sinopharm, cat. # T2008687

Milli-Q water (UP) with resistance >18.2 MΩ/cm was used throughout the experiment

Buffer Recipes

20X sodium chloride sodium citrate (SSC)	For 1 L stock solution
3 M NaCl	175.3 g NaCl
300 mM HOC(COONa)($CH_2COONa)_2 \cdot 2H2O$	88.2 g sodium citrate
pH 7.0	Adjust pH to 7.0 using HCl
	Fill up to 1L with UP
5X SSCT Hybridization buffer	For 50 mL solution
5X SSC (750 mM NaCl and 75 mM trisodium citrate)	12.5 mL of 20X SSC
0.1% Tween-20	50 μL of Tween-20
pH 7.0	Fill up to 50 mL with UP

Nupack simulation

Nupack analysis was carried out for 3 interacting DNA species (HP1, HP2 and Trigger) at 25 °C to form a maximum complex size of 3 strands.[1] Note that this setting did not adequately represent the actual interaction in solution where higher order DNA complexes might form, but sufficed in capturing the initial events of HCR and background noise formation. The reaction conditions were: Na^+ = 0.75 M and Mg^{2+} = 0.0 M with some dangle treatment.

Evaluating hairpin sequence designs using gel electrophoresis

All reactions were carried out in 5X SSCT hybridization buffer (750 mM NaCl and 75 mM trisodium citrate with 0.1% Tween-20, pH 7.0). Stock DNAs (100 μM in 1X TE, pH 8.0) were diluted to 1.5 μM separately in the hybridization buffer, heated to 95 °C for 5 min and left to cool to room temperature over at least 30 min. Equal volume of each component (three in total) was mixed to obtain the final reaction condition of 500 nM HP1 and HP2, and varying trigger concentrations. The trigger strand was pre-diluted to the required working concentration after the annealing-cooling step, i.e. if the final trigger concentration were 50 nM, the 1.5 μM stock solution was pre-diluted ten times to 150 nM. For the

negative control, i.e. 0 nM trigger concentration, the equivalent volume of hybridization buffer was added instead.

The actual sequence of addition was as follows:

1) Pre-dilute trigger strand to the required working concentration in 0.2 mL reaction tube (Thermo Scientific, cat. # AB-0620).
2) Mix the cooled 1.5 μM HP1 and HP2 working solutions together in a separate 0.2 mL tube.
3) Add 2-part of the combined hairpin mixture to 1-part trigger solution (volume basis) and vortex immediately. In this work, we added 20 μL of the hairpin mixture to 10 μL of the trigger solution.
4) Leave the reaction to proceed for 1 h at room temperature (25 °C).

All the procedures were performed at room temperature (25 °C).

Analysis was then carried out on 3% agarose gel (in 0.5X TBE buffer, pH 8.3) which was pre-stained with 1X SYBR gold nucleic acid stain. The gel was run at 90 V for 40 min in 0.5X TBE running buffer at RT.

Characterizing the optical property of dye-labelled DNA

The absorption spectrum was measured using a UV-vis spectroscopy (Varian Cary 60) and the photoluminescence spectrum was measured using a fluorescence spectrophotometer (Varian Cary Eclipse). The analysis volume was kept constant at 1 mL in Hellma semi-micro quartz cuvette (cat. # Z600768). Prior to any photoluminescent measurement, the fluorescent solution was always diluted such that the absorbance remained within 0.02 – 0.08 to avoid the inner filter effect.[2] The relative quantum yield of Cy3-HP1 was characterized using rhodamine 6G (Φ_f= 0.91 in ethanol) as the reference dye.[3]

FRET Study

All reactions were carried out in 5X SSCT hybridization buffer. Stock DNAs (100 μM in 1X TE, pH 8.0) were diluted to 1.0 μM separately in the hybridization buffer, heated to 95 °C for 5 min and left to cool to room temperature over at least 30 min. All FRET study was carried out on a microplate reader (Tecan Infinite M200). The z-position and gain was optimized using the

i-control software tool for each set of hairpin concentration and kept constant throughout the analysis. The equipment was pre-equilibrated to the reaction temperature of 25 °C, unless otherwise stated, prior to all reactions and measurements. All analysis volume was kept constant at 100 μL in 96-well black polystyrene plate (Nunc, cat. # 137101).

The actual sequence of addition was as follows:

1) Add an appropriate volume of hybridization buffer to each reaction well such that the final reaction volume is 100 μL.

2) Mix the cooled 1.0 μM HP1 and HP2 working solutions together in a separate 1.5 mL centrifuge tube.

3) Add the required volume of hairpin mixture to achieve the respective reaction concentrations. E.g. for a reaction based on 100 nM hairpin, add 20 μL of the hairpin mixture.

The FRET ratio was determined by taking the ratio of Cy3 emission (at λ_1 = 568 nm) to Cy5 emission (at λ_2 = 666 nm) at an excitation wavelength of 490 nm. The background emission was subtracted at the respective wavelengths by exciting a blank well (reaction buffer without any DNA species). The photoluminescence spectra were obtained by scanning at 530 – 800 nm (interval of 2 nm) using an excitation wavelength of 490 nm.

For the kinetic study, the microplate was inserted into the microplate reader immediately after adding all DNA components. Fluorescence measurement was performed every 1 min for a total analysis time of 60 min at an incubation temperature of 25 °C. We found that it was not necessary to correct for the effect of photobleaching over time presumably due to the ratiometric nature of FRET measurement.

For the final study on the robustness of our HCR FRET system towards biological interferences, 10 μL of FBS was added to the hybridization buffer in each well prior addition of the DNA components to obtain 10% FBS. The microplate reader was pre-equilibrated to 37 °C at which all reactions and measurements took place. All other experimental procedures remained the same as the pure DNA system.

S2. DNA Sequences Generated From Nupack Simulation [1]

Table S1. List of all DNA sequences used in this study.

Strand	Sequence
Pierce original hairpin 1 (P_HP1a)	TTA ACC CAC GCC GAA TCC TAG ACT CAA AGT AGT CTA GGA TTC GGC GTG
Pierce original hairpin 2 (P_HP2a)	AGT CTA GGA TTC GGC GTG GGT TAA CAC GCC GAA TCC TAG ACT ACT TTG
Pierce original trigger (P_Ta)	AGT CTA GGA TTC GGC GTG GGT TAA
Pierce modified hairpin 1 (P_HP1b)	TTA ACC CAC GCC GAA TCC CAA AGT GGA TTC GGC GTG
Pierce modified hairpin 2 (P_HP2b)	GGA TTC GGC GTG GGT TAA CAC GCC GAA TCC ACT TTG
Pierce modified trigger (P_Tb)	GGA TTC GGC GTG GGT TAA
New hairpin 1 (HP1c)	GGA ATT GGG AGT AAG GGC TGT GAT GCC CTT ACT CCC
New hairpin 1 with 5' Cy3 (HP1-Cy3)	/5Cy3/ GGA ATT GGG AGT AAG GGC TGT GAT GCC CTT ACT CCC
New hairpin 2 (HP2c)	GCC CTT ACT CCC AAT TCC GGG AGT AAG GGC ATC ACA
New hairpin 2 with 3' Cy5 (HP2-Cy5)	GCC CTT ACT CCC AAT TCC GGG AGT AAG GGC ATC ACA /3Cy5Sp/
New trigger (Tc)	GCC CTT ACT CCC AAT TCC
Fluorophore	GTT GGA ATT GGG AGT AAG GGC /36-FAM/
Quencher	/5IABkFQ/ GCC CTT ACT CCC

S3. Evolution of HCR Hairpin Design

We first modified the original HCR hairpin sequences reported by Pierce's group.[4] There are four key design parameters to be considered, i.e. length and CG content of hairpin stem and toehold doamins respectively. Our goal is to minimize background leakages which DNA circuits are particularly prone to. We define background leakage to be any assemblies formed from HP1 and/or HP2 in absence of the trigger strand.

First, the excessively long stem length (18 nt) could be drastically reduced to similar length as the toehold (6 nt) without appreciable background leakage according to Nupack simulation (Figure S1). The metastability of the hairpins was less sensitive to stem length than the stem CG content especially when the stem length approached that of the toehold. We found that a rough cut-off of > 60% stem CG content was effective in suppressing the background leakage.

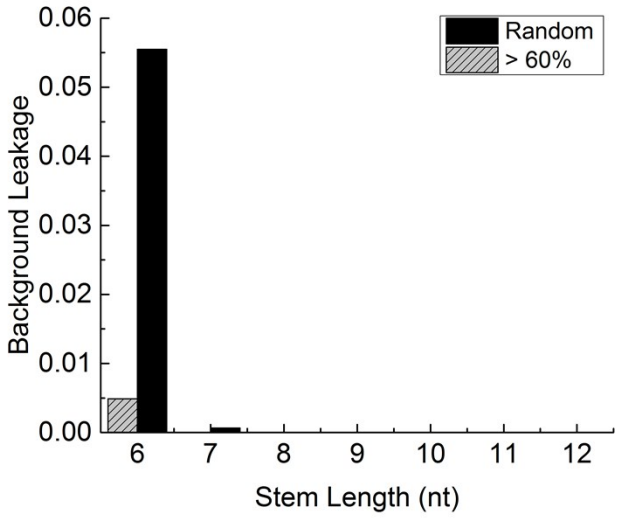

Figure S1. Effect of stem length and CG content on background leakage. Stem length is less crucial than CG content in maintaining the hairpin metastability. The toehold length was kept constant as 6 nt.

The hairpin metastability was more sensitive to the toehold properties. Generally, we noted that the CG content in the toehold should be kept below ca. 30 – 40% regardless of the toehold length (Table S2). The upper limit for the toehold length is 12 nt as recommended by Pierce's group.[5]

Otherwise, the toehold of one hairpin may form stable complex with the loop of the other hairpin with complementary domain.

Table S2. Effect of toehold length and CG content on background leakage. The stem length was kept constant at 9 nt with a CG content of 60%.

Toehold length	Toehold CG%		DNA Sequence	Leak
6	33.3	**HP1**	TTAACCGCCGAATCCCAAAGTGGATTCGGC	-
		HP2	GGATTCGGCGGTTAAGCCGAATCCACTTTG	
		T	GGATTCGGCGGTTAA	
6	50.0	**HP1**	CTAACCGCCGAATCCCAAAGTGGATTCGGC	-
		HP2	GGATTCGGCGGTTAGGCCGAATCCACTTTG	
		T	GGATTCGGCGGTTAG	
7	28.6	**HP1**	TTTAACCGCCGAATCCCAAAGTGGATTCGGC	-
		HP2	GGATTCGGCGGTTAAAGCCGAATCCACTTTG	
		T	GGATTCGGCGGTTAAA	
7	42.8	**HP1**	CTTAACCGCCGAATCCCAAAGTGGATTCGGC	+
		HP2	GGATTCGGCGGTTAAGGCCGAATCCACTTTG	
		T	GGATTCGGCGGTTAAG	
8	25.0	**HP1**	TTTTAACCGCCGAATCCCAAAGTGGATTCGGC	-
		HP2	GGATTCGGCGGTTAAAAGCCGAATCCACTTTG	
		T	GGATTCGGCGGTTAAAA	
8	50.0	**HP1**	CCTTAACCGCCGAATCCCAAAGTGGATTCGGC	+
		HP2	GGATTCGGCGGTTAAGGGCCGAATCCACTTTG	
		T	GGATTCGGCGGTTAAGG	
9	22.2	**HP1**	TTTTTAACCGCCGAATCCCAAAGTGGATTCGGC	-
		HP2	GGATTCGGCGGTTAAAAAGCCGAATCCACTTTG	
		T	GGATTCGGCGGTTAAAAA	

9	33.3	**HP1**	CTTTTAACCGCCGAATCCCAAAGTGGATTCGGC	+
		HP2	GGATTCGGCGGTTAAAAGGCCGAATCCACTTTG	
		T	GGATTCGGCGGTTAAAAG	
10	20.0	**HP1**	TTTTTTAACCGCCGAATCCCAAAGTGGATTCGGC	+
		HP2	GGATTCGGCGGTTAAAAAAGCCGAATCCACTTTG	
		T	GGATTCGGCGGTTAAAAA	

S4. Robustness of Design Rules under Different Experimental Conditions

We validated the robustness of our newly-generated HCR hairpin sequences under different experimental conditions. All reactions were carried out according to the "Evaluating hairpin sequence designs using gel electrophoresis" protocol, except for the modification of specific experimental condition as stated for each study.

NaCl concentration

We selected three buffer systems commonly used for HCR studies which contained 140 mM,[6] 500 mM[4] and 750 mM[5] NaCl respectively to evaluate the effect of NaCl concentration. From Figure S2, it is evident that both the positive signal (lanes 2 – 4, 6 – 8 and 10 – 12) and background leakage (lanes 1, 5 and 9) had similar profiles. In particular, there was no noticeable circuit leakage even at the high NaCl concentration of 750 mM NaCl for 500 nM hairpins.

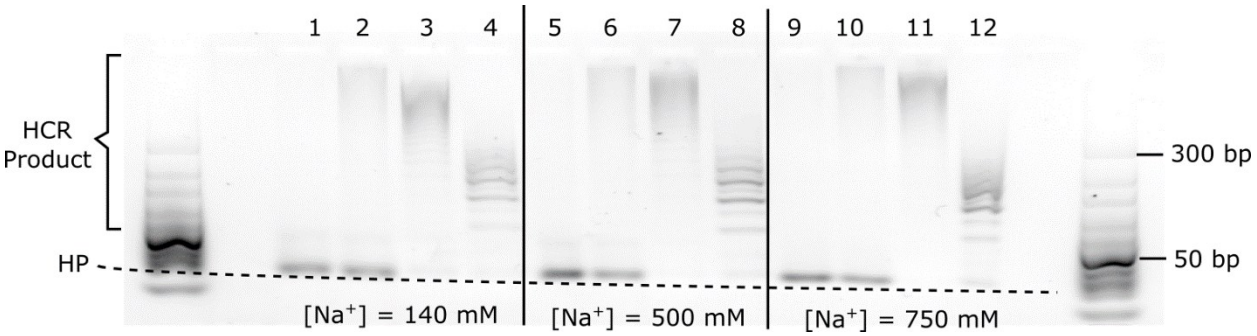

Figure S2. Gel image demonstrating the effect of NaCl concentration on the HCR hairpin metastability. Different buffers of varying NaCl concentration commonly encountered in HCR studies were used: 1X PBS (pH 7.4) (Lanes 1 – 4), 50 mM H_2PO_4 (pH 6.8) and 500 mM NaCl (Lanes 5 – 8) and 5X SSCT (Lanes 9 – 12). For each buffer system, trigger concentration of (from left to right) 0x, 0.01x, 0.1x and 1.0x that of 500 nM HP1c and HP2c was used. The reaction mixture was incubated at 25 °C for 1 h. A 10 – 300 bp DNA ladder is shown on both sides of the gel.

$MgCl_2$ concentration

We fixed the base buffer system as 1X PBS (pH 7.4) which is most commonly used especially for biological studies and spiked three concentrations of $MgCl_2$, i.e. 5 mM,[7] 10 mM[8] and 12.5 mM,[9]

to evaluate the effect of $MgCl_2$ concentration. We again observed good signal development with no noticeable circuit leakage even at the high $MgCl_2$ concentration of 12.5 mM for 500 nM hairpins (Figure S3).

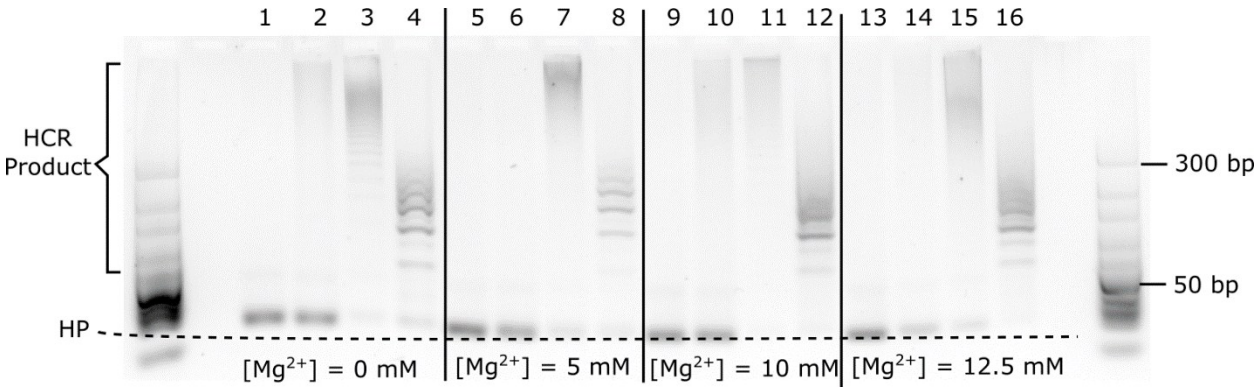

Figure S3. Gel image demonstrating the effect of $MgCl_2$ concentration on the HCR hairpin metastability. 1X PBS (pH 7.4) spiked with varying $MgCl_2$ concentration commonly encountered in HCR studies were used: 0 mM $MgCl_2$ (Lanes 1 – 4), 5.0 mM $MgCl_2$ (Lanes 5 – 8), 10.0 mM $MgCl_2$ (Lanes 9 – 12) and 12.5 mM $MgCl_2$ (Lanes 13 – 16). For each buffer system, trigger concentration of (from left to right) 0x, 0.01x, 0.1x and 1.0x that of 500 nM HP1c and HP2c was used. The reaction mixture was incubated at 25 °C for 1 h. A 10 – 300 bp DNA ladder is shown on both sides of the gel.

Reaction temperature

We incubated 500 nM hairpins with the respective target concentrations in 5X SSCT hybridization buffer at three different temperatures of 4 °C, 25 °C and 37 °C. Higher temperature was not attempted. From Figure S4, the generation of positive signal was reduced slightly when the temperature was lowered. This was most obvious for the case of 0.01x trigger concentration (lane 2 versus 6). Slight circuit leakage was observed at 37 °C (lane 9), though it should be noted that the generation of positive signal was promoted to a larger extent (lane 10 versus 6). Hence the net effect was an improvement in the signal-to-noise ratio (lane 10 over 9), which was still a favourable outcome for target detection or visualization.

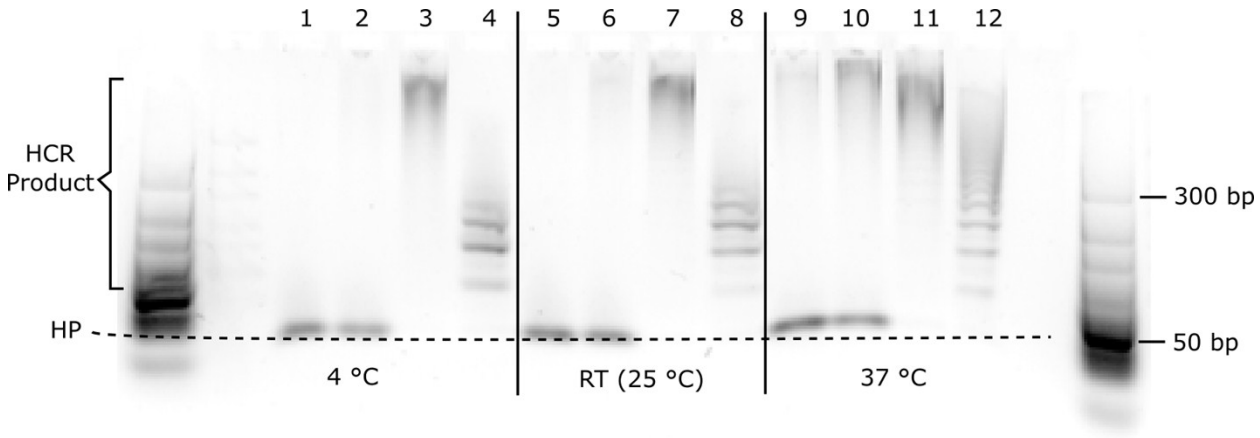

Figure S4. Gel image demonstrating the effect of temperature on the HCR hairpin metastability: 4 °C (Lanes 1 – 4), room temperature of 25 °C (Lanes 5 – 8) and 37 °C (Lanes 9 – 12). For each temperature, trigger concentration of (from left to right) 0x, 0.01x, 0.1x and 1.0x that of 500 nM HP1c and HP2c was used. The hybridization buffer used was 5X SSCT. The reaction mixture was incubated for 1 h. A 10 – 300 bp DNA ladder is shown on both sides of the gel.

Hairpin concentration

Higher hairpin concentration should result in a more severe problem of circuit leakage due to the higher probability of spurious hybridization. We had tested our hairpin sequences at 5 nM, 20 nM, 100 nM (FRET readout) and 500 nM (gel readout) concentration in the main text. Here, we tested our HCR system at an even higher hairpin concentration of 1000 nM (lanes 9 – 12) which still remained metastable in absence of trigger strand (lane 9) (Figure S5). By comparing three representative hairpin concentrations of 100 nM (lanes 1 – 4), 500 nM (lanes 5 – 8) and 1000 nM, we observed that the profile of the HCR product formed was largely dependent on the trigger-to-hairpin ratio rather than the absolute trigger concentration used. This was similarly deduced from our HCR FRET sytem discussed in the main text and further supported the usefulness of HCR as a tool for controlled amplification.

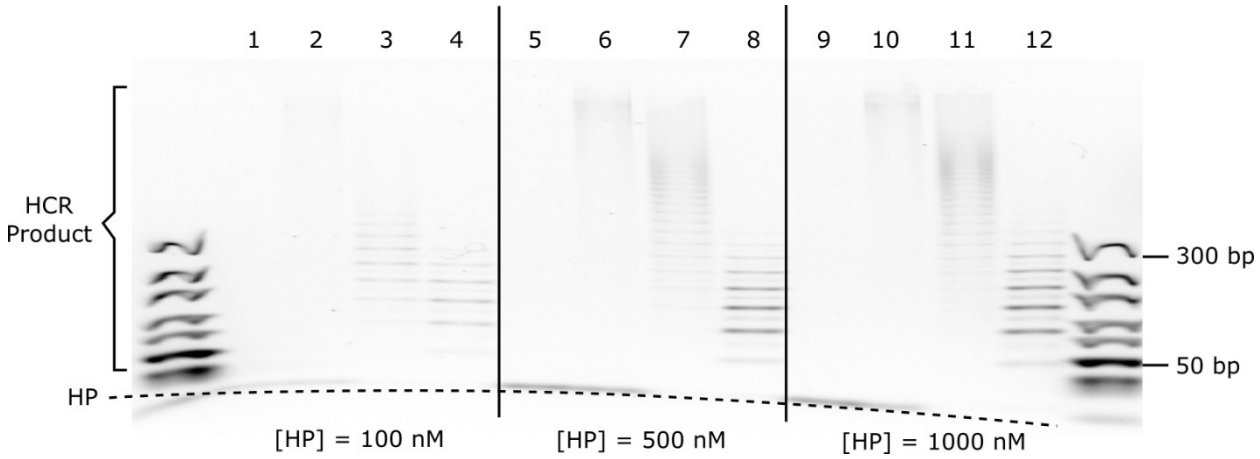

Figure S5. Gel image demonstrating the effect of HCR hairpin (HP) concentration on its metastability: [HP] = 100 nM (Lanes 1 – 4), [HP] = 500 nM (Lanes 5 – 8) and [HP] = 1000 nM (Lanes 9 – 12). For each HP concentration, trigger concentrations of (from left to right) 0x, 0.01x, 0.1x and 1.0x that of the respective HP concentration were used. The hybridization buffer used was 5X SSCT. The reaction mixture was incubated at 25 °C for 1 h. A 10 – 300 bp DNA ladder is shown on both sides of the gel.

S5. Deviation from Design Guidelines

Based on our experimental experience, deviations from the general design guidelines introduced in this work often resulted in detectable levels of background leakages using gel electrophoresis. We highlight two examples here.

In the first example shown in Figure S6, hairpins with the same structure as Pierce's design,[4] *i.e.* 6 nt toehold length and 18 nt stem length, were designed using Nupack web server.[1] We picked the first set of randomly-generated sequences which coincidentally had notably higher toehold CG% than our recommended range of 30 – 40%. Shorter HCR products formed which indicated the increased efficiency of HCR triggering. The input hairpins were almost completely consumed even at a low trigger concentration of 10 nM (Lane 5). The higher signal production was unfortunately accompanied by significant background leakage (Lane 6). Readers may notice that the stem CG% was also lower than our recommended >60% cut-off. It is worth pointing out at this point that Pierce's original design had the same stem CG% of 55.6%. This was consistent with our experimental observations to date that the stem CG% was a less crucial factor when the hairpin stem was significantly longer than, *i.e.* a heuristically derived cut-off of two times, the toehold length.

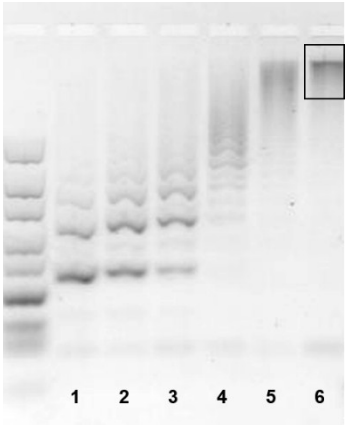

Strand	Sequence	Toehold CG%	Stem CG%
HP1	GAT GAG GGT AGT GAG GGT GAG ATG GGC TTG CAT CTC ACC CTC ACT ACC	50.0	55.6
HP2	CAT CTC ACC CTC ACT ACC CTC ATC GGT AGT GAG GGT GAG ATG CAA GCC	66.7	55.6
Trigger	CAT CTC ACC CTC ACT ACC CTC ATC	-	-

Figure S6. Gel electrophoresis image when hairpins of 18 nt stem length and 6 nt toehold length were used. Lanes 1 – 5 represent decreasing trigger concentration of 1000 nM, 500 nM, 100 nM, 50 nM and 10 nM. Lane 6 represents the negative control when 1000 nM of HP1 and HP2 reacted in absence of trigger strand. The background leakage is indicated by the black box. A 10 – 300 bp DNA ladder is shown on the left-hand side of the gel. The DNA sequences and corresponding toehold / stem CG % are shown in the right-hand side table.

In the second example shown in Figure S7, hairpins with the same structure as our newly generated sequences described in the main text, *i.e.* 6 nt toehold length and 12 nt stem length, were designed using Nupack web server, except that the toehold CG% of HP1 exceeded our recommended 30 – 40% cut-off. The addition of one CG base pair led to detectable level of background leakage (Lane 4). There was a marginal increase in the background leakage, as indicated by increased HCR product intensity and reduced hairpin band intensity, when the temperature increased from 4 °C (Lane 3) to 37 °C (Lane 5). On the other hand, our hairpin sequences remained robust to background leakage even when challenged at higher temperature (Lane 10).

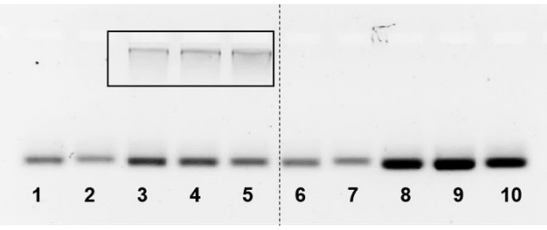

Strand	Sequence	Toehold CG%	Stem CG%
HP1	GGA AGT GGG AGT AAG GGC TGT GAT GCC CTT ACT CCC	50.0	66.7
HP2	GCC CTT ACT CCC ACT TCC GGG AGT AAG GGC ATC ACA	33.3	66.7
Trigger	GCC CTT ACT CCC ACT TCC	-	-

Figure S7. Gel electrophoresis image when hairpins of 12 nt stem length and 6 nt toehold length were used. Lanes 1 – 5 contain the hairpin sequences shown on the table to the right. Lanes 1 and 2 represent 500 nM of HP1 only and HP2 respectively. Lanes 3 – 5 represent 500 nM of HP1 + HP2 at 4 °C, room temperature (25 °C) and 37 °C respectively. The background leakage is indicated by the black box. Lanes 6 – 10 are identical set-ups as Lanes 1 – 5 but using the hairpin sequences described in the main text.

S6. Evaluating Kinetics of Shorter Stem Length Design

To evaluate the kinetics of HCR, we developed a simple method to quench the reaction at different time points. The idea was to terminate the elongation of the HCR chain by blocking the single-stranded active domains using complementary protector strands (P1 and P2) (Figure S8). For example, P1 hybridized to unreacted trigger strand (T) to stop further HCR triggering. Also, the growing ends of the HCR chain was blocked by P2 and P1 at the single-stranded ends of HP1 and HP2 respectively.

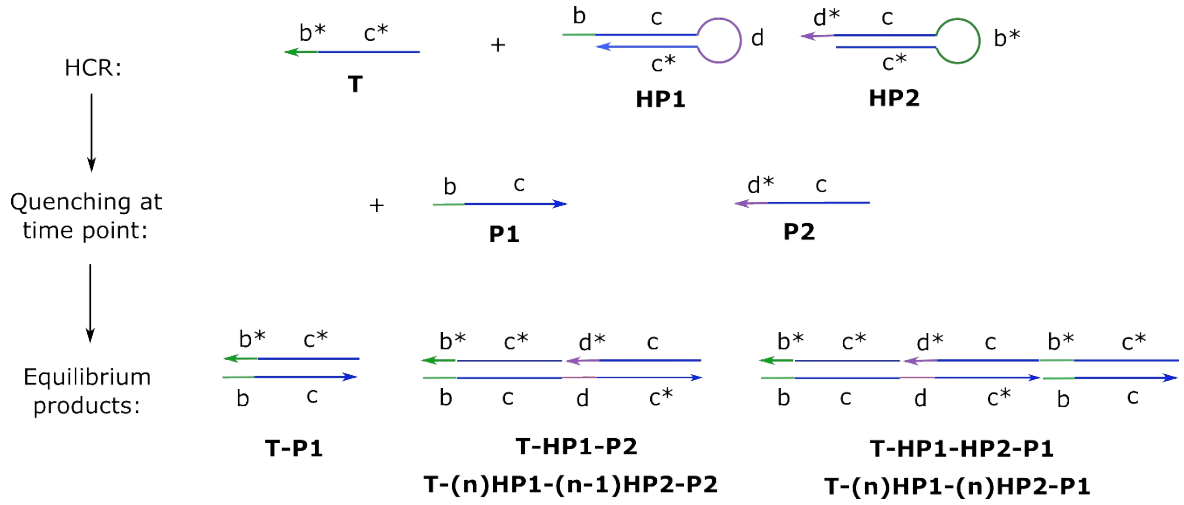

Figure S8. Reaction schematic to evaluate the kinetics of HCR. Protector strands (P1 and P2) were added to the reaction mixture at respective time points to quench the reaction. These strands were designed to be complementary to the active domains of the trigger strand and growing HCR chain. The equilibrium products obtained belong to three main classes: 1) quencher trigger strand (T-P1), 2) quenched HP1 active end and 3) quenched HP2 active end. The growing HCR chain could be terminated at different chain lengths (denoted as n in the scheme).

We compared the kinetics of our new sequence design (toehold = 6 nt, stem = 12 nt) and Pierce's original sequence (toehold = 6 nt, stem = 18 nt) using the method presented in Figure S8.[4] 500 nM of HP1 and HP2 were reacted with 10 nM of T which were quenched at respective time points using two times molar ratio (200 nM) of P1 and P2. Gel electrophoresis was used to visualize the results (Figure S9). As the reaction progressed with time, two key observations could be made, i.e. the intensity of the hairpin bands diminished while the average length of the HCR product increased.

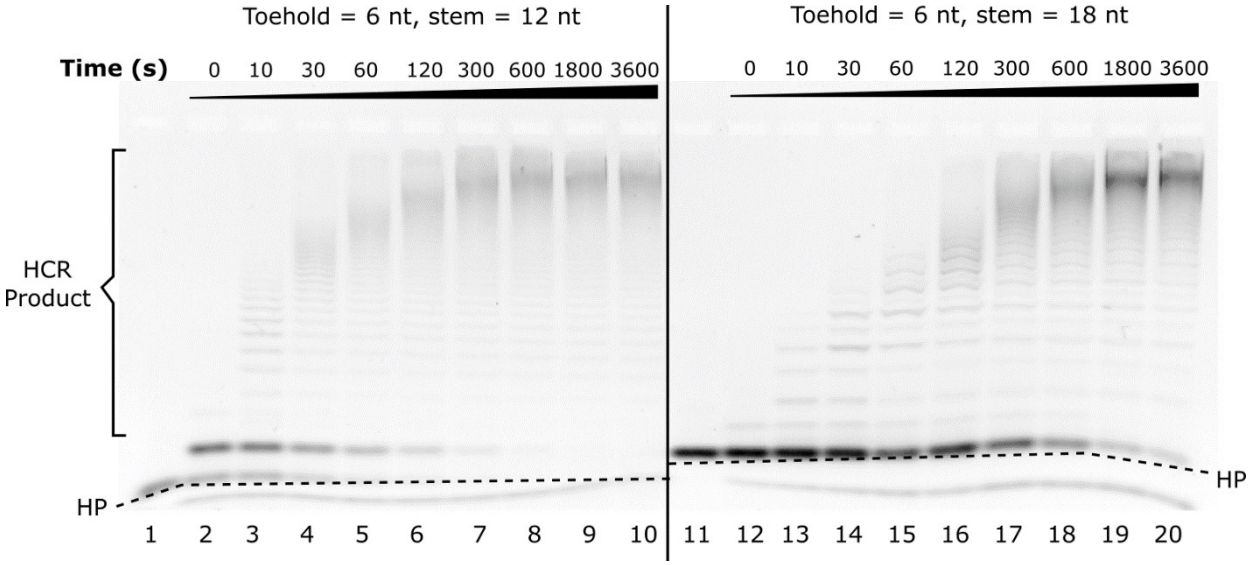

Figure S9. Evolution of the HCR product over time for our hairpin design (lanes 1 – 10) and Pierce's design (lanes 11 – 20) on 3% agarose gel pre-stained with 1X Sybr gold. Lanes 1 and 11 represent 100 nM HP1c and HP2c. Lanes 2 and 12 represent 100 nM HP1 + HP2 + 200 nM P1 + P2. The reaction mixture (100 nM HP1 + HP2 + 10 nM T), represented by Lanes 3 – 10 and Lanes 13 – 20, was quenched at the time point indicated on top of the respective lanes using the method shown in Figure S8.

The intensities of the hairpin bands were quantified using ImageJ and normalized to the equivalent concentration values.[10] The kinetics data were fitted using a pseudo first-order reaction kinetics since the hairpin concentration (100 nM) was greater than the trigger strand (10 nM) (Figure S10). We wish to point out that this simple data analysis did not fully capture all the complex kinetics involved in HCR and the competing P1 and P2 strands. However, the black box format did describe the system adequately for us to arrive at a semi-quantitative conclusion. The rate constant for our sequence was 0.0116 s^{-1} which was ca. 10 times faster than that of Pierce's sequence ($k' = 0.00115\ s^{-1}$). This could be due to the faster kinetics involved in opening a hairpin with shorter stem length due to its weaker metastability and shorter branch migration length.

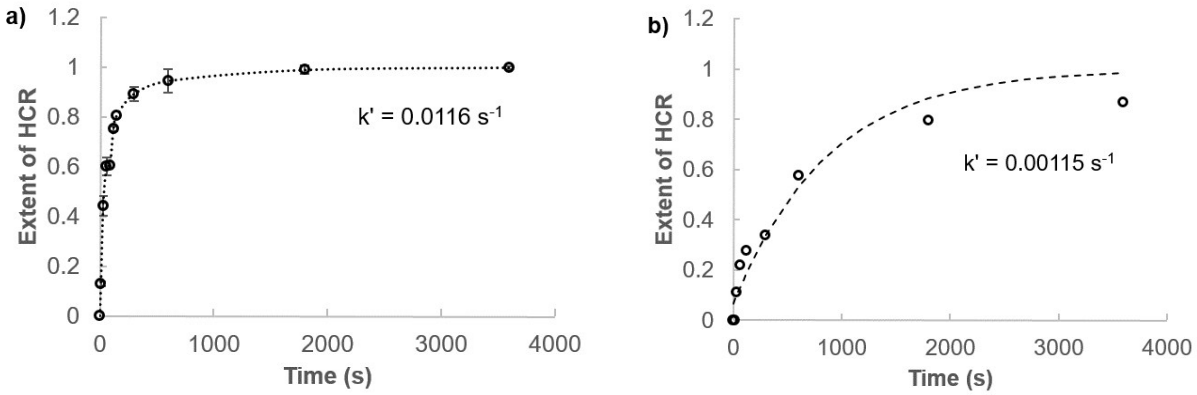

Figure S10. Kinetics profile of (a) our newly generated hairpin sequences (toehold = 6 nt, stem = 12 nt) and (b) Pierce's original hairpin sequences (toehold = 6 nt, stem = 18 nt) expressed in terms of the extent of HCR. The data was quantified from the gel image in Figure S9. The apparent rate constant of our design (k' = 0.0116 s^{-1}) is ca. 10 times greater than that of Pierce's (k' = 0.00115 s^{-1}) which could be attributed to the faster kinetics involved in opening hairpins of shorter stem length.

S7. Evaluating Förster Resonance Energy Transfer (FRET) Properties

Förster resonance energy transfer (FRET) refers to the nonradiative energy transfer from an excited donor molecule (Cy3) to an acceptor molecule (Cy5) due to their spectral overlap (Figure S11).[11] It is described by the Förster radius (R_o) which is the center-to-center separation distance (r) where the energy transfer efficiency is 50%. This parameter was calculated using equation **1**.

$$R_o = (B\ \Phi_D\ I)^{1/6} \qquad (\mathbf{1})$$

where, B and I were calculated using equations **2** and **3** respectively.

Φ_D = quantum yield of Cy3 (determined to be 0.277 using rhodamine 6G as reference dye)

$$B = \frac{9000[\ln(10)]\kappa_p^2}{128\pi^5 n_D^4 N_A} \qquad (\mathbf{2})$$

where, κ_p^2 = dipole orientation factor (range from 0 – 4; in this case, $\kappa = 2/3$ for the randomly oriented dipole);

n_D = refractive index (1.33 for water);

N_A = Avogadro's number.

The overlap integral, I, measures the extent of spectral overlap between the donor and acceptor dipole and is described by equation **3** and plotted in Figure S12a.

$$I = \int_0^\infty PL_{D\text{ - }corr}(\lambda)\ \epsilon_A(\lambda)\ \lambda^4\ d\lambda \qquad (\mathbf{3})$$

Where, ε_A = acceptor absorption spectrum;

$PL_{D\text{-}corr}$ = normalized donor emission spectrum.

Solving for I gives 8.31×10^{15} M^{-1} cm^{-1} nm^4.

Substituting back to equation **1** gives $\mathbf{R_o = 56.9\ Å}$.

The average energy transfer efficiency (E) was calculated using equation **4**,

$$E = \frac{(F_D - F_{DA})}{F_D} \quad (\mathbf{4})$$

where F_D and F_{DA} are the fluorescence intensities of Cy3 only (donor) and Cy3 in presence of Cy5 (acceptor).

E can also be calculated theoretically based on the Förster dipole-dipole formalism expressed in equation **5**,

$$E = \frac{n R_0^6}{n R_0^6 + r^6} \quad (\mathbf{5})$$

where n is the average number of Cy5 acceptor per Cy3 donor molecule.

In our HCR FRET system, each Cy3 molecule has two Cy5 neighbors along the one-dimensional DNA assembly, suggesting that n = 2 (D-2A). At the same time, each Cy5 molecule has two Cy3 neighbors as well for the energy transfer process and possibly possesses only 50% probability of accepting the energy from either Cy3 neighbor. In this case, n = 1 (D-A). The simulation results of the two scenarios are shown in Figure 12b. For a fixed separation distance of ca. 61.2 Å, the single donor-acceptor energy transfer model can better describe the maximum E value of 0.382 obtained experimentally.

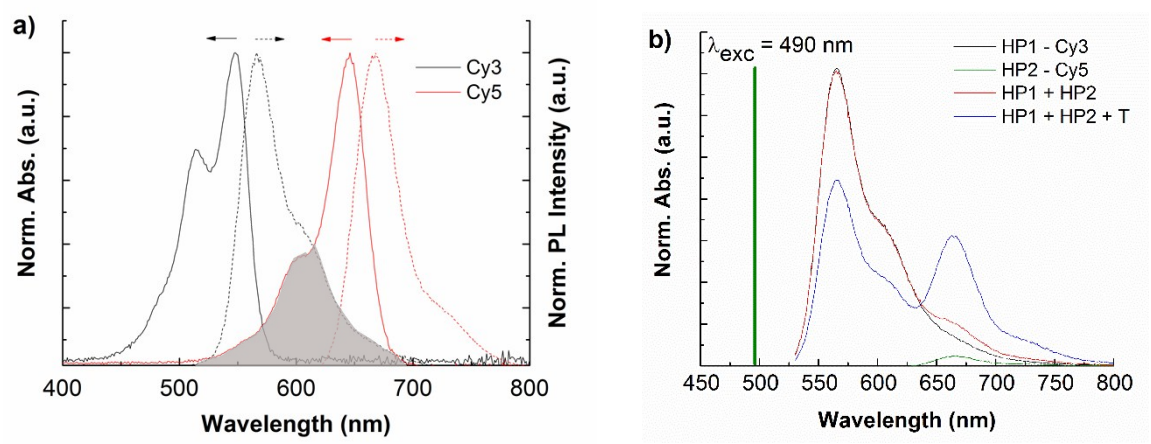

Figure S11. (a) Normalized absorbance (solid line) and emission (dotted line) spectrum of HP1-Cy3 (black) and HP2-Cy5 (red). Energy transfer took place within the overlap region (grey). (b) At the excitation wavelength (λ_{exc}) of 490 nm, there was minimal emission from Cy5-HP2 (green line) while Cy3-HP1 (black line) generated high fluorescence emission. A mixture of Cy3-HP1 and Cy5-HP2 resulted in obvious FRET in the presence of the trigger strand (blue line) as compared to the significantly lower background noise in absence of the trigger strand (red line).

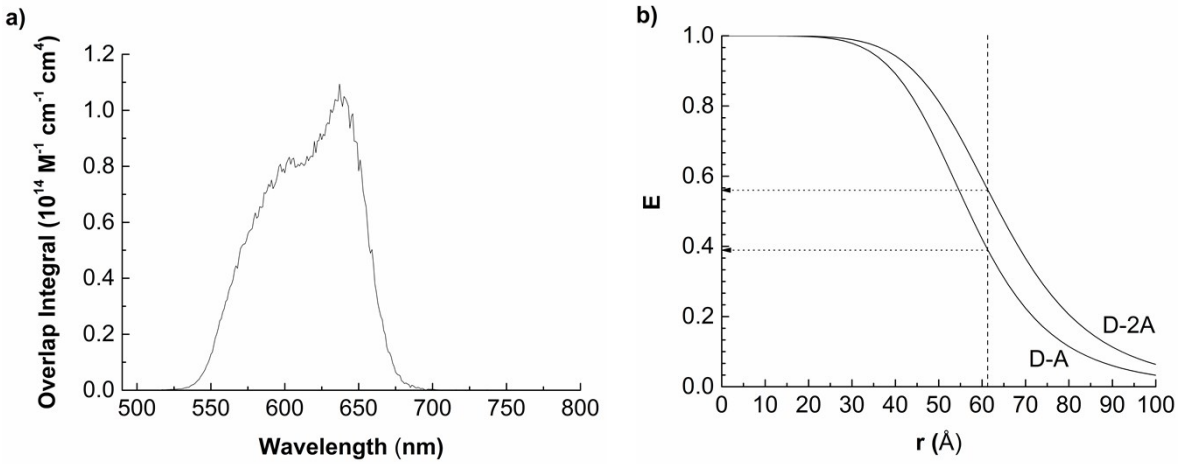

Figure S12**.** (a) The overlap integral curve was used to calculate the Förster distance (R) as 56.9 Å. (b) The simulated FRET efficiency (E) was plotted for both single donor-acceptor pair (D-A) and donor-double acceptor pair (D-2A). The experimental E obtained was 0.382 for a fixed separation distance (r) of ca. 61.2 Å (dotted line) which can be better explained by a single donor-acceptor pair (D-A) than a two acceptors model (D-2A).

S8. Further Characterization of the HCR FRET System

We further characterized the reaction kinetics (Figure S13a and Table S3) and FRET readout (Figure S13b) when [HP] = 5.0 nM.

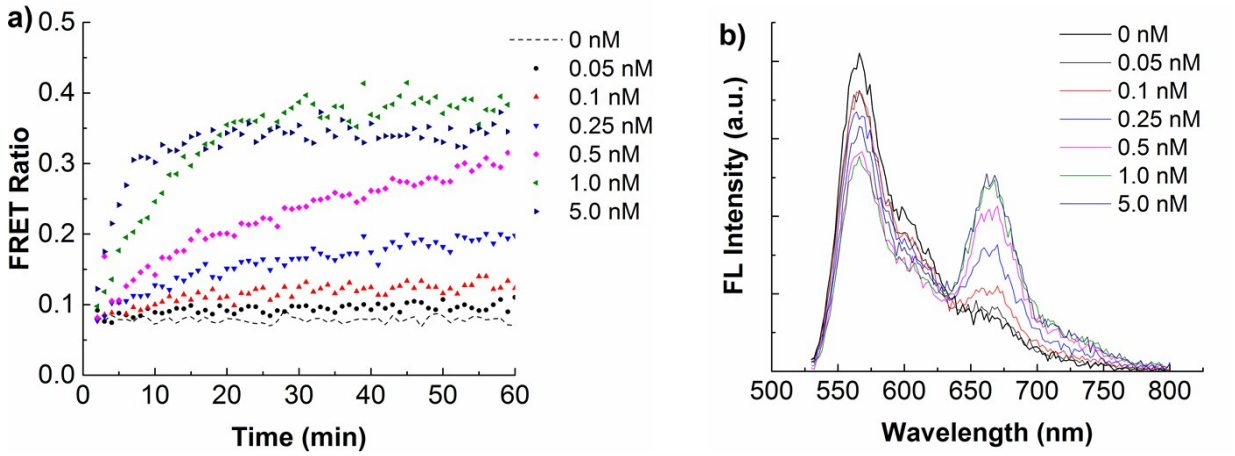

Figure S13. (a) Kinetics profile of HCR FRET for [HP] = 5.0 nM at different trigger concentrations. Note that the results were plotted from 2 min onwards to account for the lag time due to mixing and measurement initialization. (b) As the trigger concentration increased from 0 nM to 5.0 nM, the fluorescence intensity of Cy3-HP1 decreased while that of Cy5-HP2 increased which indicated the dosage dependence of the FRET process. [HP] = 5.0 nM.

Table S3. Initial reaction rate of the HCR FRET system when [HP] = 5.0 nM.

[Trigger] (nM)	**Initial Rate, k_{ini} (10^{-9} M min^{-1})**
0	0.99
0.05	1.06
0.1	1.08
0.25	1.31
0.5	1.58
1	2.44
5	3.37

References

1 J. N. Zadeh, C. D. Steenberg, J. S. Bois, B. R. Wolfe, M. B. Pierce, A. R. Khan, R. M. Dirks and N. A. Pierce, *J. Comput. Chem.*, 2011, **32**, 170.

2 Y. S. Ang and L. Y. L. Yung, *Nanoscale*, 2014, **6**, 12515.

3 C. Würth, M. Grabolle, J. Pauli, M. Spieles and U. Resch-Genger, *Nat. Protoc.*, 2013, **8**, 1535.

4 R. M. Dirks and N. A. Pierce, *Proc. Natl. Acad. Sci. U. S. A.*, 2004, **101**, 15275.

5 H. M. T. Choi, V. A. Beck and N. A. Pierce, *ACS Nano*, 2014, **8**, 4284.

6 X. Chen, *J. Am. Chem. Soc.*, 2012, **134**, 263.

7 M. You, L. Peng, N. Shao, L. Zhang, L. Qiu, C. Cui and W. Tan, *J. Am. Chem. Soc.*, 2014, **136**, 1256.

8 Y. Tang, Z. Wang, X. Yang, J. Chen, L. Liu, W. Zhao, X. C. Le and F. Li, *Chemical Science*, 2015, **6**, 5729.

9 C. Wu, S. Cansiz, L. Zhang, I. T. Teng, L. Qiu, J. Li, Y. Liu, C. Zhou, R. Hu, T. Zhang, C. Cui, L. Cui and W. Tan, *J. Am. Chem. Soc.*, 2015, **137**, 4900.

10 C. A. Schneider, W. S. Rasband and K. W. Eliceiri, *Nat. Meth.*, 2012, **9**, 671.

11 A. R. Clapp, I. L. Medintz, J. M. Mauro, B. R. Fisher, M. G. Bawendi and H. Mattoussi, *J. Am. Chem. Soc.*, 2004, **126**, 301.